



## STRUCTURAL, MORPHOLOGICAL AND THERMAL ANALYSIS OF NaCMC /HPC/MnO<sub>2</sub> POLYMERNANOFILMS SYNTHESIZED BY USING SOLUTION CASTING TECHNIQUE

Mannala SRIDEVI,<sup>a</sup> Uppara NARESH,<sup>b\*</sup> Rapole JEEVAN KUMAR<sup>a\*</sup> and Talluri RAMPRASAD<sup>c</sup>

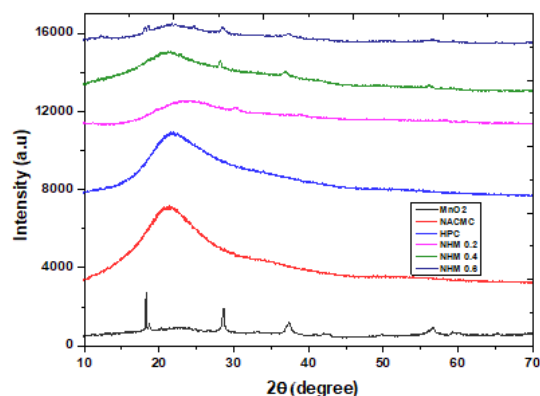
<sup>a</sup>Sri Krishnadevaraya University, Anantapur, A.P, India-515001

<sup>b</sup>Rajiv Gandhi University of Knowledge and Technology, R.K Vally. A.P, India-516330

<sup>c</sup>St. Peters Engineering College, JNTU- Hyderabad, Telangana, India-50010

Received November 2, 2024

In our research, we created nanocomposite samples using a blend of sodium carboxymethyl cellulose (NaCMC), hydroxypropyl cellulose (HPC), and manganese dioxide (MnO<sub>2</sub>) nanoparticles. We used the solution casting technique to synthesise these polymer nanocomposite samples, with the key component being a 50/50 blend of hydroxypropyl cellulose and carboxymethyl cellulose as the organic host matrix. By adding different concentrations of 0.2, 0.6, and 0.8 per cent of MnO<sub>2</sub> nanoparticles named NHM 0.2, NHM 0.4, and NHM 0.6. We used XRD, FTIR, DSC and SEM techniques to analyse the structural and morphological properties of the samples. The FTIR spectra confirmed the blend through the formation of hydrogen bond interaction and showed the interaction between the polymer and nanoparticles. X-ray diffraction (XRD) analysis revealed that the pure blend was amorphous. SEM images displayed bright spots on the sample surfaces, which were attributed to the presence of MnO<sub>2</sub> nanoparticles. DSC curves demonstrated decreased glass transition and melting point temperatures for the nanocomposite samples. These nanocomposites exhibit unique and intriguing properties, showing promise for practical applications in various applications. Our research inspires the potential of this field and the practical implications of our findings.



### INTRODUCTION

Polymer blending is a fundamental process in materials science that involves mixing two or more different polymers to create new materials with enhanced properties.<sup>1</sup> A polymer blend is a macroscopically homogeneous mixture of two or more polymers (homopolymers or copolymers) that have been blended to create a new material with different physical properties.<sup>1</sup> This technique has

gained significant importance in polymer science due to its theoretical and practical implications.<sup>1</sup>

Sodium carboxymethyl cellulose (NaCMC) and hydroxypropyl cellulose (HPC) are important cellulose derivatives used in various industries. Blending these polymers has gained attention, especially in materials science and pharmaceutical formulations.

Sodium carboxymethyl cellulose is an anionic, water-soluble polyelectrolyte derived from

\* Corresponding author: nareshkk@gmail.com

cellulose. It is synthesised by reacting alkali cellulose with sodium monochloroacetate under controlled conditions. The degree of substitution (DS) in NaCMC, which refers to the average number of hydroxyl groups substituted per glucose unit, significantly influences its properties and applications.

NaCMC exhibits high solubility in water at all temperatures, forming clear solutions. Its solubility is directly related to its degree of substitution. The pure form of NaCMC presents as a white or milk-white fibrous powder or particles characterised by being odourless and tasteless. It is insoluble in organic solvents, distinguishing it from other cellulose derivatives.

Hydroxypropyl cellulose is an ether of cellulose in which some hydroxyl groups in the repeating glucose units have been hydroxypropylated, forming  $-OCH_2CH(OH)CH_3$  groups using propylene oxide. The degree of substitution (DS) for HPC can reach up to 3, with the moles of substitution (MS) potentially exceeding this value due to the reactivity of the added hydroxypropyl groups.

HPC is unique among cellulose derivatives due to its solubility in water and polar organic solvents. It exhibits a lower critical solution temperature (LCST) at approximately 45 °C, below which it is readily soluble in water. The pH range of HPC solutions typically falls between 5.0 and 8.5, making it suitable for a wide range of applications.

The blending of NaCMC and HPC is driven by the desire to combine their unique properties. NaCMC, with its excellent water solubility, thickening properties, and the ability to form strong gels, is a significant contributor. HPC, on the other hand, provides good film-forming characteristics and organic solvent solubility. This combination allows for developing materials with improved mechanical properties, controlled release profiles, and enhanced functionality. Various techniques can be used to blend NaCMC and HPC, including solution blending, melt blending, solution casting technique and reactive blending.

Characterizing NaCMC/HPC blends typically involves combining techniques to assess their physical, chemical, and mechanical properties. Fourier Transform Infrared Spectroscopy (FTIR) is used to identify functional groups and potential interactions between the polymers. Differential Scanning Calorimetry (DSC) was employed to

study the thermal behaviour and miscibility of the blends. Scanning Electron Microscopy (SEM) was utilised to examine the morphology and phase distribution in the blended materials.

**Applications of NaCMC/HPC Blends**  
NaCMC/HPC blends find extensive applications in the pharmaceutical sector, particularly in controlled drug delivery systems. These blends are used in formulating matrix tablets to modulate drug release profiles. The combination of NaCMC and HPC allows for the development of pH-sensitive drug delivery systems, taking advantage of NaCMC's pH-dependent solubility.

**Recent Advancements in NaCMC/HPC Blending, Nanocomposite Blends**  
Recent research has focused on incorporating nanoparticles into NaCMC/HPC blends to enhance their properties further. For instance, adding halloysite nano clay to NaCMC/HPC blend membranes has improved their thermal stability and mechanical properties.

There is a growing interest in developing more sustainable and environmentally friendly NaCMC/HPC blends. This includes exploring bio-based additives and optimising blend compositions to minimise environmental impact while maintaining desirable performance characteristics. While NaCMC/HPC blends offer numerous advantages, several challenges remain in their development and application, which include **Compatibility Issues**; ensuring optimal compatibility between NaCMC and HPC across various blend ratios and processing conditions remains a significant challenge. **Processing Limitations**: some blending techniques, particularly those involving high temperatures, can degrade the polymers, affecting the blend's final properties. **Regulatory Considerations**: As these blends find increased use in pharmaceutical and food applications, addressing regulatory requirements and ensuring consistent quality becomes crucial.

Blending sodium carboxymethyl cellulose (NaCMC) and hydroxypropyl cellulose (HPC) represents a significant area of research and development in polymer science. Combining the unique properties of these two cellulose derivatives makes it possible to create materials with enhanced functionality, improved performance characteristics, and a wide range of applications across various industries. As research advances, we can expect the development of increasingly sophisticated NaCMC/HPC blends that address specific

challenges in drug delivery, food technology, and materials science. The ongoing exploration of novel blending techniques, incorporation of nanomaterials, and focus on sustainability will likely drive further innovation in this exciting area of polymer science, inspiring new directions and applications.<sup>1-9</sup>

Sodium carboxymethyl cellulose (NaCMC) and hydroxypropyl cellulose (HPC) are versatile cellulose derivatives that have gained significant attention in materials science and engineering. Blending these polymers with manganese dioxide (MnO<sub>2</sub>) nanoparticles has emerged as a promising avenue for developing advanced composite materials with enhanced properties and multifunctional capabilities. MnO<sub>2</sub> nanoparticles can be synthesised through various methods, including co-precipitation and green synthesis approaches. One notable green synthesis method involves using lemon extract as a reducing agent and curcumin as a stabilising agent. This environmentally friendly approach allows the production of MnO<sub>2</sub> nanoparticles with controlled size and stability, which is crucial for effective blending with NaCMC and HPC.

Various blending techniques, including solution blending, in-situ synthesis, and melt blending, can integrate MnO<sub>2</sub> nanoparticles with NaCMC and HPC. Several factors influence the properties of NaCMC/HPC/MnO<sub>2</sub> nanocomposites. Loading of MnO<sub>2</sub> nanoparticles significantly impacts the composite's mechanical, thermal, and functional properties. The molecular weight of NaCMC and HPC affects the viscosity and film-forming properties of the blend. For NaCMC and HPC, the degree of substitution influences their solubility and interaction with MnO<sub>2</sub> nanoparticles. Parameters such as temperature, pH, and mixing time play crucial roles in determining the final properties of the nanocomposite.

The introduction of MnO<sub>2</sub> nanoparticles into NaCMC and HPC matrices has been demonstrated to enhance various mechanical properties. These enhancements include increased tensile strength, stiffer materials due to higher Young's modulus, and improved flexural strength in nanocomposites containing MnO<sub>2</sub>. Additionally, including MnO<sub>2</sub> nanoparticles notably alters the thermal behaviour of NaCMC and HPC.

The thermal stability of NaCMC and HPC is generally improved when blended with MnO<sub>2</sub> nanoparticles. The presence of MnO<sub>2</sub> nanoparticles can influence the glass transition temperature of the

polymer matrix, impacting its processability and mechanical properties at various temperatures. MnO<sub>2</sub> nanoparticles can also enhance the thermal conductivity of the composite, which could be advantageous for applications needing effective heat dissipation.

Various functional properties have been discovered in blends of NaCMC and HPC, including the incorporation of MnO<sub>2</sub> nanoparticles. The introduction of MnO<sub>2</sub> nanoparticles has been found to enhance the electrochemical behaviour, significantly improving the composite's electrochemical properties. This makes it suitable for energy storage applications such as supercapacitors. Additionally, research indicates that antimicrobial properties in NaCMC and HPC blends containing MnO<sub>2</sub> nanoparticles have shown potential for medical applications. However, the development and application of NaCMC and HPC blends with MnO<sub>2</sub> nanoparticles face challenges in achieving uniform dispersion, enhancing interface interactions, ensuring scalability, and maintaining long-term stability.

These nanocomposites exhibit enhanced mechanical strength, improved thermal stability, and novel functional properties that make them suitable for various applications, from water purification to energy storage and biomedical devices. While challenges remain in optimising these materials' synthesis, dispersion, and long-term stability, ongoing research and development efforts pave the way for their increased adoption in various industrial sectors. As understanding of the fundamental interactions between cellulose derivatives and MnO<sub>2</sub> nanoparticles continues to grow, we can expect the emergence of even more sophisticated and high-performance nanocomposites tailored for specific technological needs.<sup>10</sup>

Cheo *et al.*<sup>15</sup> developed a novel nanoparticle screening technique to enhance aceclofenac's solubility and oral bioavailability. Sodium carboxymethylcellulose (Na-CMC) showed the most significant increase in drug solubility. Different nanoparticle systems were prepared and evaluated, with the nano-emulsifying drug delivery system (SNEDDS) showing the highest bioavailability of aceclofenac. This technique could be a valuable tool for improving the solubility and bioavailability of poorly water-soluble bioactive materials.

Akalin *et al.*<sup>16</sup> developed a novel nanoparticle screening technique to enhance the solubility and bioavailability of aceclofenac. Various solid

dispersion and self-emulsifying drug delivery systems were evaluated, with the solid self-nano emulsifying drug delivery system (SNEDDS) exhibiting the highest bioavailability. This technique shows potential for improving the properties of poorly water-soluble bioactive materials.

Kitahara *et al.*<sup>17</sup> examined Hydroxypropyl cellulose (HPC) as a potentially effective material for thermoresponsive nanogels. Cholesterol-modified HPC (Ch-HPC) created nano gels through hydrophobic interactions in water and demonstrated a lower critical solution temperature than native HPC. The size of Ch-HPC nano gels could be reversibly modified through temperature changes and salting-out effects, like Ch-HPC-cross-linked microgels, underscoring its promise in thermoresponsive applications.

Junior *et al.*<sup>18</sup> conducted a study on microfibrillated cellulose (MFC) and hydroxypropyl methylcellulose (HPMC) as gelling agents in hydroalcoholic solutions. They explored the interactions between MFC and cellulose derivatives in organic solvents, creating phase diagrams and performing rheological measurements. Their results indicated that ethanol significantly impacts the rheological properties of the dispersions, and urea tests further illuminated the types of interactions present within the systems.

Kokol *et al.*<sup>19</sup> studied the effects of adding water-soluble polymers, hydroxyethyl cellulose (HEC) and carboxymethyl cellulose (CMC) to microfibrillated cellulose (MFC) suspensions. They found that these polymers enhanced MFC's flow rigidity, water retention, and rheological properties while lowering viscosity and improving suspension stability. Elżbieta *et al.*<sup>20</sup> studied how surfactants affect the adsorption of carboxymethylcellulose (NaCMC) on manganese dioxide (MnO<sub>2</sub>). They found that surfactants increased NaCMC adsorption by forming complexes with the polymer. Importantly, surfactant adsorption was independent of NaCMC's initial concentration, and higher pH levels led to decreased NaCMC adsorption. Additionally, the presence of NaCMC and surfactants reduced MnO<sub>2</sub>'s surface charge density and zeta potential.

The importance of these studies reflects influence across multiple disciplines with individual and combination NaCMC, HPC, and MnO<sub>2</sub> nanoparticles. Improving these combinations may be helpful in drug delivery systems, boosting environmental cleanup methods, and aiding agricultural advancements and energy

applications; research on NaCMC/HPC/MnO<sub>2</sub> nanoparticles is leading to innovative solutions for numerous global issues. The interdisciplinary aspect of this research underscores its ability to connect various scientific areas, promoting collaborations that may result in groundbreaking technologies and applications soon. Hence, Hear. The NaCMC/HPC/MnO<sub>2</sub> composite was prepared using the solution casting technique aiming to investigate the structural, morphological, and thermal stability of the prepared composites using the X-ray diffraction (XRD), Fourier-transform infrared spectroscopy (FTIR), scanning electron microscopy (SEM), differential scanning calorimetry (DSC), and thermogravimetric analysis (TGA) to analyse the properties of the composites.

## EXPERIMENTAL

In this study, we utilised hydroxypropyl cellulose (HPC) with a molecular weight of 125,000 in its analytical grade, sourced from Merck India Ltd., as well as the sodium salt of carboxymethylcellulose (NaCMC) acquired from Loba Chem in Mumbai, India. These materials were the foundational components for preparing HPC/NaCMC/MnO<sub>2</sub> nanocomposite films. The films were created using the solution casting technique, a method known for its effectiveness in producing uniform and high-quality film structures.

### 1. Preparation of NaCMC solution

To prepare the sodium carboxymethyl cellulose (NaCMC) solution, 4 grams of high-purity NaCMC polymer were carefully measured using an analytical balance to ensure accuracy. This polymer was then added to 100 ml of deionised water, chosen for its lack of impurities that could interfere with the experimental results.

The mixture was placed in a clean glass beaker and subjected to continuous stirring using a magnetic stirrer set at a moderate speed. This stirring process was maintained for approximately 24 hours to facilitate the thorough dissolution of the NaCMC and achieve a uniform, smooth solution free of lumps or undissolved particles.

The temperature was monitored throughout this period to avoid excessive heating, which could degrade the polymer. Once a clear and homogenous solution was obtained, it was carefully transferred

to a suitable container for use in subsequent miscibility studies.

## 2. Preparation of HPC solution

To prepare the Hydroxypropyl Cellulose (HPC) solution, the process began by accurately weighing the appropriate amount of HPC powder using a digital balance. Then, the HPC was added to 100 ml of deionised water in a beaker. The mixture was stirred continuously with a magnetic stirrer to ensure thorough dispersion of the HPC in the water. This stirring process continued for approximately 24 hours, allowing ample time for the HPC to dissolve and ultimately form a smooth, uniform solution.

Once the solution reached consistency, it was carefully diluted to ensure its volume and concentration aligned with the sodium carboxymethyl cellulose (NaCMC) solution. This step was essential for maintaining the accuracy of subsequent calculations and experiments involving both polysaccharides.

## 3. Preparation of NaCMC/HPC blend films:

A homogeneous solution composed of sodium carboxymethyl cellulose (NaCMC) and hydroxypropyl cellulose (HPC) was prepared with a concentration exceeding that used in previous experiments while maintaining a consistent ratio of 25:25. This preparation involved continuous stirring to ensure complete mixing of the components, resulting in a uniform solution.

Once the mixture reached the desired consistency, it was carefully transferred to a ceramic plate. The plate was then placed in a controlled environment at ambient temperature to facilitate the evaporation of water from the solution. Over 24 hours, the water gradually evaporated, leaving behind a solid film of the blended materials.

After the entire evaporation period, the resulting films were meticulously peeled off the ceramic plate. This careful process yielded films of the appropriate thickness, ready for further analysis or application.

## 4. Preparation of NaCMC/HPC/MnO<sub>2</sub> nanocomposite films:

The NaCMC/HPC/MnO<sub>2</sub> nanocomposite films were fabricated using the solution casting technique, which is known for its effectiveness in producing homogeneous materials. The prepared mixture consisted of sodium carboxymethyl cellulose (NaCMC) and hydroxypropyl cellulose (HPC) in

equal ratios of 25 grams each. This mixture was continuously stirred to ensure complete dissolution and a stable, homogeneous solution.

Following this, a series of manganese dioxide (MnO<sub>2</sub>) suspensions, each with varying concentrations, were prepared to explore their effects on the nanocomposite properties. The concentrations of MnO<sub>2</sub> used were 0.2 g, 0.4 g, and 0.6 g. Additionally, suspensions labelled NHM 0.2, NHM 0.4, and NHM 0.6 were made for comparative analysis using ultrasonication for 1 hour. This ultrasonic treatment was crucial as it facilitated the dispersion of MnO<sub>2</sub> particles, preventing agglomeration and ensuring an even distribution throughout the solution.

Once the MnO<sub>2</sub> suspensions were prepared, they were integrated into the NaCMC/HPC solution. The combined solution was then cast onto a flat ceramic plate, which provided a non-stick surface ideal for film formation. The casting process involved spreading the solution evenly to achieve a uniform thickness across the film.

The ceramic plate was left undisturbed at ambient temperature for 24 hours to promote drying, allowing the water content to evaporate completely. This evaporation process was instrumental in solidifying the composite structure by allowing the polymer matrix to encapsulate the dispersed MnO<sub>2</sub> particles.

After fully evaporating water, the resultant nanocomposite films were carefully removed from the ceramic plate. The removal process was executed gently to avoid damaging the movie and to maintain its desired thickness and structural integrity. The final product showcased a series of nanocomposite films, each exhibiting distinct properties based on the concentration of MnO<sub>2</sub> used during fabrication.

# RESULTS AND DISCUSSION

## 1. XRD results

Figure 1 is a graphical representation of X-ray diffraction (XRD) patterns for materials currently studied that are measured as a function of the scattering angle. This curve represents the XRD pattern for manganese dioxide (MnO<sub>2</sub>), which typically exhibits specific peaks corresponding to its crystalline structure.

This curve NaCMC indicates the XRD pattern for Sodium Carboxymethylcellulose (NaCMC). Due to its amorphous nature, it shows a different

pattern from crystalline materials. Similarly, The Hydroxypropyl Cellulose (HPC) curve also demonstrates an amorphous character, with characteristic peaks that differ from those of  $\text{MnO}_2$ .

These curves likely represent different formulations or concentrations of composite materials NHM 0.2, NHM 0.4, and NHM 0.6. The differing intensities and peak positions indicate changes in the mixtures' crystallinity or structural characteristics.

The position of peaks in the XRD pattern provides information about the d-spacing and crystal structure of the materials. Well-defined peaks suggest crystalline materials, whereas broad peaks or a lack of distinct peaks indicate amorphous materials. The changes in intensity among different samples can indicate variations in concentration, crystallinity, or interactions between components (like NaCMC and  $\text{MnO}_2$ ) in composite materials.

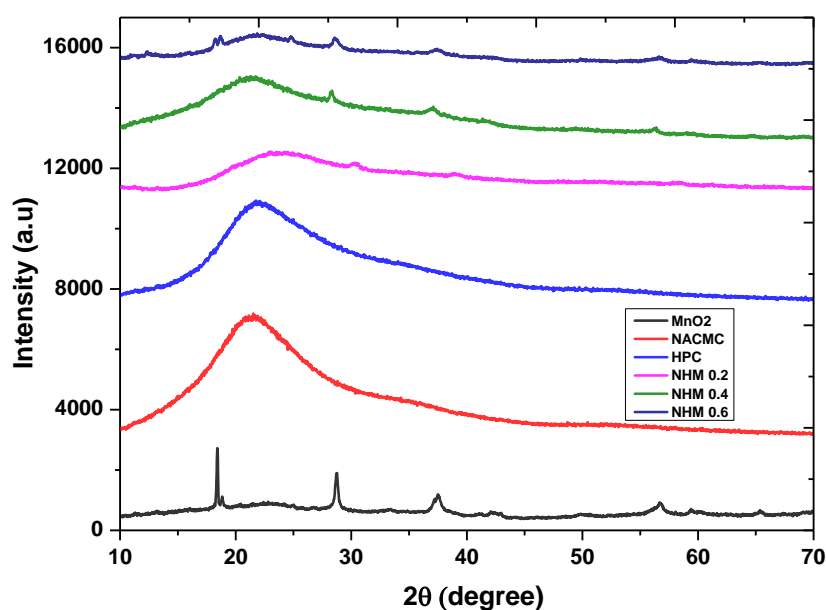


Fig. 1 – XRD spectrum for pure NaCMC, HPC crystal structures of  $\text{MnO}_2$  Nps.

In the X-ray diffraction (XRD) spectra presented in Fig. 1, we observe distinct characteristics of the studied materials. The spectrum for Hydroxypropyl cellulose (HPC) and NaCMC reflects the amorphous structure, with two well-defined sharp peaks at  $23.6^\circ$ , corresponding to the (112) and (120) planes, as referenced in.<sup>1,5,14</sup> In contrast, the XRD spectrum for pure Sodium carboxymethyl cellulose (NaCMC) displays a broad peak at  $2\theta = 18.3^\circ$ , suggesting the amorphous nature of NaCMC. Moving on to the crystal structures of Manganese dioxide nanoparticles ( $\text{MnO}_2$  Nps) in Fig. 1a, we observe Bragg reflection patterns at  $2\theta = 38.1^\circ$  (111),  $44.2^\circ$  (200),  $64.8^\circ$  (220), and  $77.3^\circ$  (311), which are characteristic of the face-centred cubic (fcc) structure of  $\text{MnO}_2$  Nps.

## 2. SEM results

The surface morphological study of  $\text{MnO}_2$  doped NaCMC-HPC blend composite films was carried

out for pure  $\text{MnO}_2$ , pure blend, 2 wt %, 4 wt % and 6 wt % of NaCMC-HPC - $\text{MnO}_2$  films, and the results are shown in Fig. 2.

Figure 2 illustrates that the pure  $\text{MnO}_2$  nanoparticles are spherical and contain agglomerated particles. In contrast, the pure NaCMC-HPC blend exhibits a smooth surface. When  $\text{MnO}_2$  nanoparticles are incorporated into the polymer blend matrix, the surface morphology of the films changes with increasing doping concentrations (2 and 3 wt%). Specifically, the 2 wt% composite films shown in Fig. 2c show a notable increase in surface roughness compared to the pure blend. This roughness continues to increase in the 3 wt% composite films depicted in Fig. 2d. The observed enhancement in surface crystallinity and roughness of the composite films is expected to contribute positively to their conductivity, as evidenced by the conductivity measurements.<sup>23</sup>



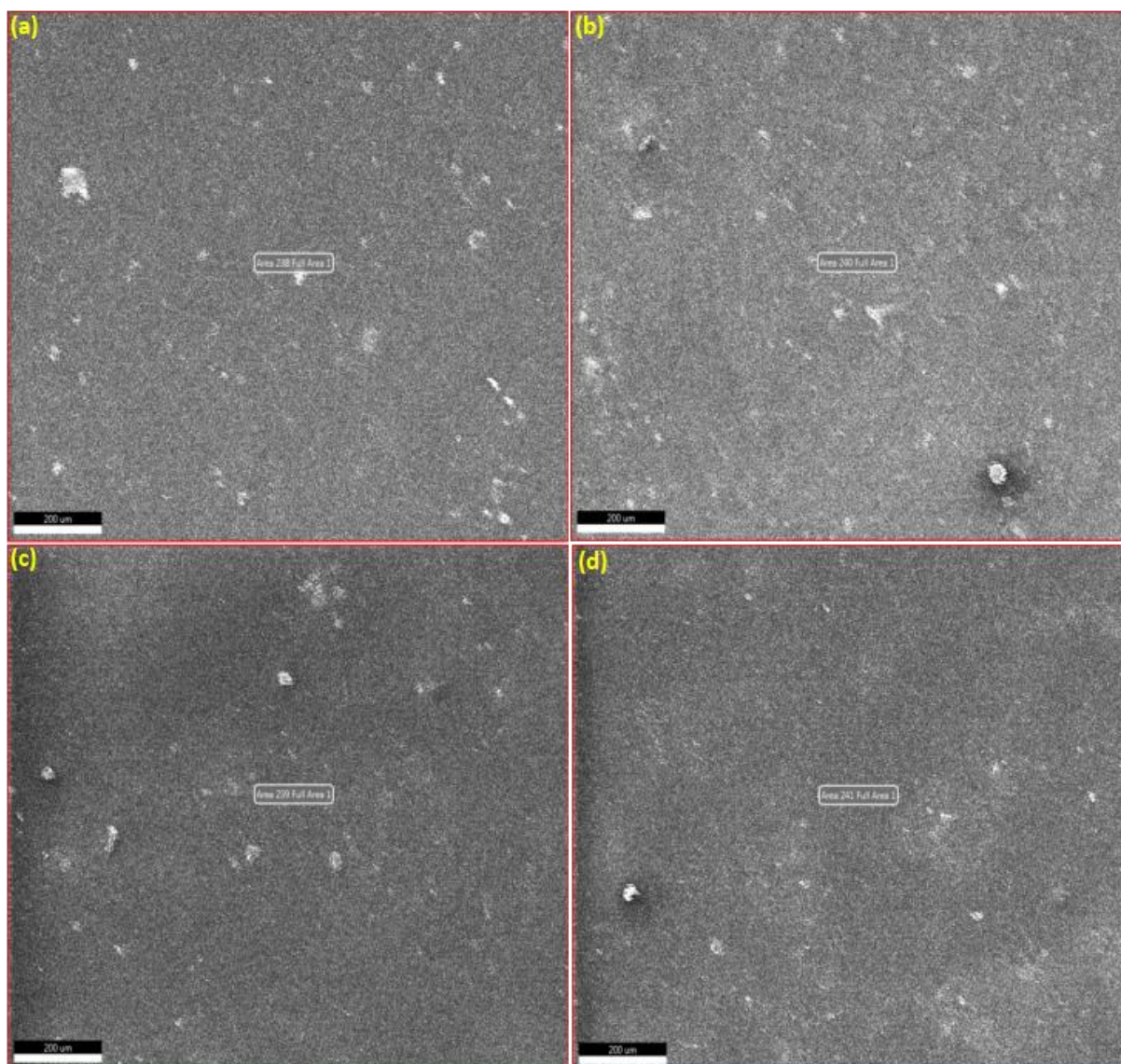


Fig. 2 – SEM Images of NaCMC, HPC crystal structures of MnO<sub>2</sub> Nps.

### 3. FTIR results

The FTIR spectra of pure MnO<sub>2</sub>-doped NaCMC-HPC blends are displayed in Fig. 3. The figure shows that the O-H stretching vibrations band is observed around 3445 cm<sup>-1</sup> for the pure NaCMC/HPC polymer blend. The weak bands at 2922 and 2851 cm<sup>-1</sup> correspond to the asymmetric and symmetric stretching vibrations of C-H, respectively, and the band at 1742 cm<sup>-1</sup> corresponds to C=O stretching. The band at 1652 cm<sup>-1</sup> is attributed to the stretching vibrations of C=C (aromatic) of HPC, and the bands corresponding to C-H bending and C-O stretching vibrations are observed at 1470 and 1085 cm<sup>-1</sup>, respectively. For the composite films, these bands are shifted from 3445, 2922, 2851, 1742, 1652, and 1740 cm<sup>-1</sup> to

3341, 2939, 2830, 1733, and 1636 cm<sup>-1</sup>, respectively, and new bands are observed at 530 and 694 cm<sup>-1</sup>. These new bands are attributed to the stretching vibrations of Mn-O and O-Mn-O. The bending of NaCMC and HPC results in four types of polymer-polymer interactions: van der Waals, hydrophobic, electrostatic, and hydrogen bonding. Within the blend matrix, the present group of the NaCMC chain and a hydroxy group of the HPC chain are expected. The nanoparticles MnO<sub>2</sub> interact with the carboxyl and OH groups, forming a complex with the blend, which modifies the chemical structures and, hence, the physical and chemical properties. The complex formation occurs cooperatively, resulting in compact structures, which are reflected in changes in the intensities in some IR bands, and new bands arise on doping.<sup>24</sup>

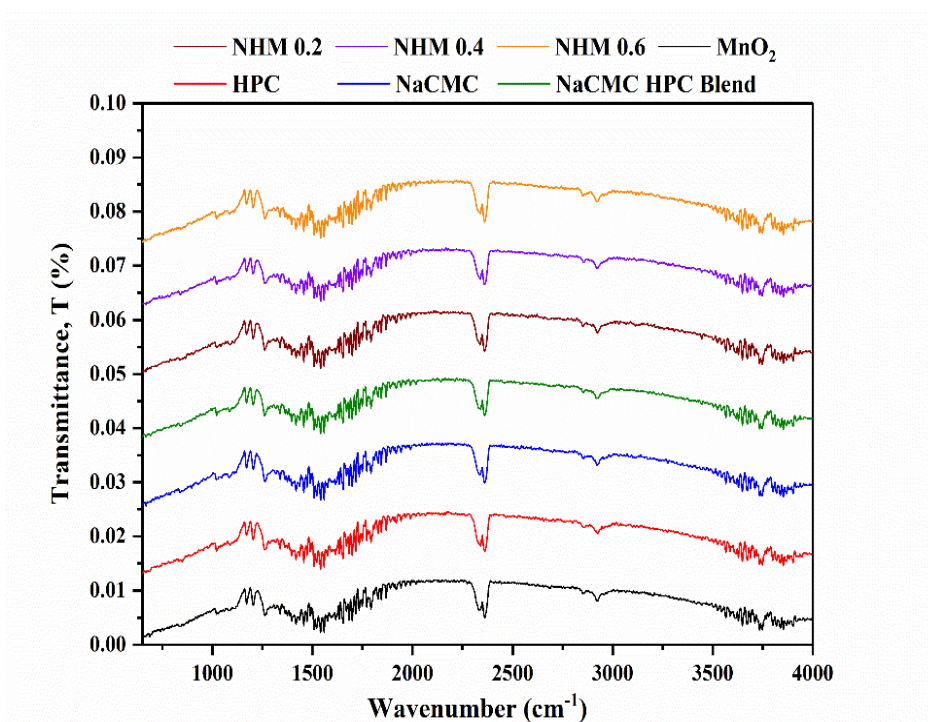


Fig. 3 – XRD spectrum for pure NaCMC, HPC crystal structures of MnO<sub>2</sub> Nps.

#### 4. Thermal analysis

Figure 4 represents a differential scanning calorimetry (DSC) analysis, where the heat flow is measured as a function of temperature for different samples ranging from 50 °C to 600 °C. The Pure MnO<sub>2</sub>,

the curve likely represents the thermal behaviour of pure manganese dioxide, showing a relatively stable heat flow with minor changes. Meanwhile, for NHM 0.2, NHM 0.4, and NHM 0.6, these curves represent samples with varying concentrations of composite material, denoted by NHM.

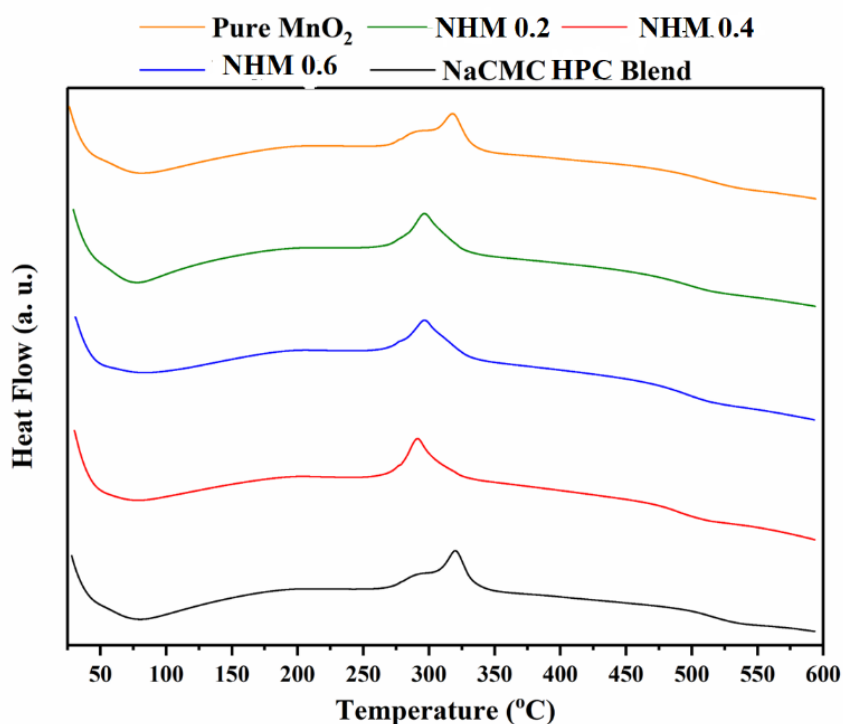


Fig. 4 – DSC analysis of the prepared samples.



Each curve displays different thermal characteristics, suggesting how the percentage of NPM affects heat flow and thermal stability. As well as for NaCMC Blend. This curve depicts the behaviour of a blend made from sodium carboxymethyl cellulose (NaCMC) and polyvinyl alcohol (PVA), indicating its heat flow properties during the heating process. The differences in the shapes and positions of the curves indicate varied thermal properties of the samples. Peaks or valleys in the heat flow curves may suggest phase transitions such as melting or crystallization. In essence, this graph helps analyse the thermal

properties of different materials, which can significantly influence their applications in fields like materials science and engineering.

The provided thermogravimetric analysis (TGA) graph in Fig. 5 illustrates the weight loss profiles of various samples as a function of temperature, ranging from 50 to 600 °C. The graph represents the percentage weight of the materials, spanning from 20% to 110%, with the initial weight indicated at approximately 100% before thermal degradation. At approximately 200 °C, all samples exhibit stable weight retention, remaining close to their initial values.

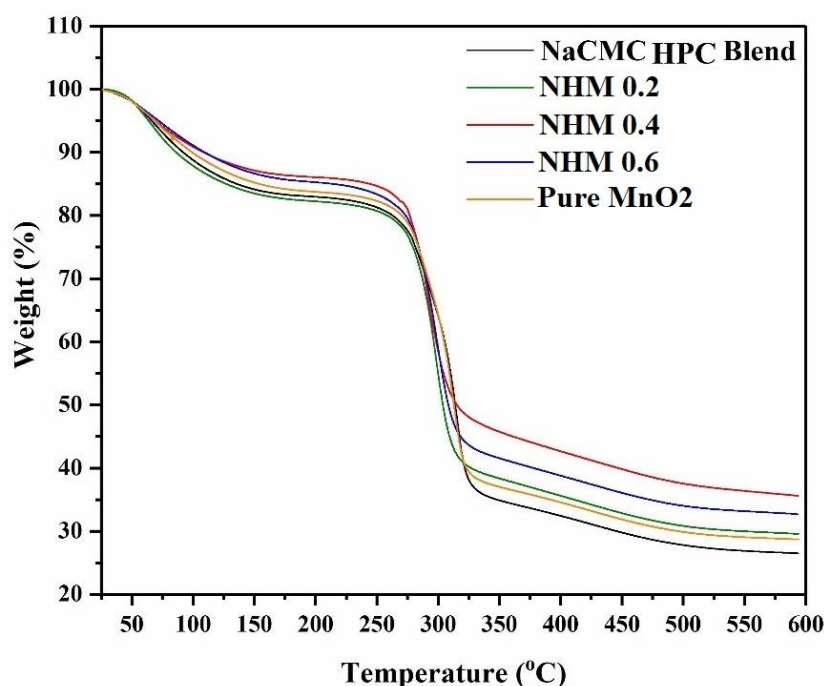


Fig. 5 – DSC-TGA analysis of a sample.

Exceeding this temperature threshold, there is a pronounced weight loss indicative of thermal degradation mechanisms at play, with variations in both the degree and rate of loss among the samples. Specifically, samples labelled NHM 0.2, 0.4, and 0.6 demonstrate distinct thermal stability and degradation characteristics. Additionally, Pure MnO<sub>2</sub> showcases a unique thermal behaviour compared to the blends of NaCMC and HPC and the NPM samples.

This analysis is integral to evaluating materials' thermal stability, especially in the context of battery technology, advanced materials science, and polymer composites. The differential weight loss profiles provide critical insights into the materials' performance and suitability under specific operational conditions.<sup>25</sup>

## CONCLUSION

This study illustrates that the introduction of MnO<sub>2</sub> particles into the NaCMC/HPC host matrix significantly enhances the performance of the composite blend membrane compared to the unfilled NaCMC/HPC. However, elevated concentrations of MnO<sub>2</sub> lead to increased rigidity of the NaCMC/HPC matrix, resulting in a decrease in flux while simultaneously improving selectivity toward water. Characterization of the resulting membranes via FTIR, DSC, TGA, SEM, and XRD assessments indicates that they possess sufficient thermal and mechanical stability and favourable surface-free energy-key attributes for effective pervaporation dehydration at temperatures above ambient conditions.

## REFERENCES

1. S. Li, Y.-M. Liu, Y.-C. Zhang, Y. Song, G.-K. Wang, Y.-X. Liu, Z.-G. Wu, B.-H. Zhong, Y.-J. Zhong, and X.-D. Guo, *J. Power Sources*, **2021**; <https://doi.org/10.1016/j.jpowsour.2020.229331>.
2. V. S. Kulkarni and C. Shaw, *Essential Chemistry for Formulators of Semisolid and Liquid Dosages*, **2016**; <https://doi.org/10.1016/b978-0-12-801024-2.00005-4>.
3. C. G. Lopez, S. E. Rogers, R. H. Colby, P. Graham and J. T. Cabral, *J. Polymer Sci. Part B: Polymer Phys.*, **2014**; <https://doi.org/10.1002/polb.23657>.
4. H. S. Wahyuni, S. Yuliasmi, H. S. Aisyah and D. Riati, *Open Access Macedon. J. Medical Sci.*, **2019**; <https://doi.org/10.3889/oamjms.2019.524>.
5. Md. S. Rahman, Md. S. Hasan, A. S., Nitai, S. Nam, A. K. Karmakar, Md. S. Ahsan, M. J. A. Shiddiky and M. B. Ahmed, *Polymers*, **2021**; <https://doi.org/10.3390/polym13081345>.
6. V. Mikušová, J. Ferková, D. Žigayová, D. Krchňák and P. Mikuš, *Gels*, **2022**; <https://doi.org/10.3390/gels8030168>.
7. R. Garduque, B. Gococo, C. Yu, P. Nalzarro and T. Tumolva, *Solid State Phenomena*, **2020**, *304*, 51–57; [10.4028/www.scientific.net/SSP.304.51](https://doi.org/10.4028/www.scientific.net/SSP.304.51).
8. R. N. Oliveira and G. B. McGuinness, *Polymers and Polymeric Composites: A Reference Series*, **2018**; <https://doi.org/10.1007/978-3-319-76573-039-1>.
9. H. Dardeer, A. Gad and M. Mahgoub, *BMC Chemistry*, **2024**, *18*; [10.1186/s13065-024-01244-w](https://doi.org/10.1186/s13065-024-01244-w).
10. A. T. Mekuria, *J. Nanotechnol. Nanomater.*, **2024**; <https://doi.org/10.33696/nanotechnol.5.052>.
11. E. Grządka, *J. Surfactants and Detergents*, **2012**, *15*, 513–521; [10.1007/s11743-012-1340-5](https://doi.org/10.1007/s11743-012-1340-5).
12. A. T. Mekuria, *J. Nanotechnol. Nanomater.*, **2024**; <https://doi.org/10.33696/nanotechnol.5.052>.
13. L. Oliveira, S. Bennici, L. Josien, L. Limousy, M. Bizeto and F. Camilo, *Carbohydrate Polymers*, **2019**, 115621; [10.1016/j.carbpol.2019.115621](https://doi.org/10.1016/j.carbpol.2019.115621).
14. Q. N. Tran, T. N. Vo, I. T. Kim, J. H. Kim, D. H. Lee and S. J. Park, *Materials*, **2021**; <https://doi.org/10.3390/ma14216619>.
15. S. Cheon, J. S. Kim, M. R. Woo, S. H. Ji, S. Park, F. Ud Din, J. O. Kim, Y. S. Youn, K. T. Oh, S. J. Lim, S. G. Jin, J. E. Chung and H. G. Choi, *Int. J. Biol. Macromol.*, **2024**, *277*, 134246; doi: [10.1016/j.ijbiomac.2024.134246](https://doi.org/10.1016/j.ijbiomac.2024.134246). Epub 2024 Aug 4. PMID: 39098461.
16. M. Akalin, O. Gulen and M. Pulat, *J. Nanomater.*, **2018**, 9676949. Accessed September 26, 2024; <https://doi.org/10.1155/2018/9676949>.
17. Y. Kitahara, M. Sakiyama, S. Takeda, T. Nishimura, S.-A. Mukai, S.-I. Sawada, Y. Sasaki and K. Akiyoshi, *Langmuir, ACS J. Surfaces Colloids.*, **2016**, *32*; [10.1021/acs.langmuir.6b02406](https://doi.org/10.1021/acs.langmuir.6b02406).
18. E. Junior, A. Lucizani, V. Veríssimo, C. Pires, A. Andrade, M. Matos, G. Perissutti, W. Magalhães and R. de Freitas, *Cellulose*, **2024**, *31*, 7925–7940; [10.1007/s10570-024-06085-3](https://doi.org/10.1007/s10570-024-06085-3).
19. V. Kokol, *Cellulose*, **2022**, *29*; [10.1007/s10570-022-04737-w](https://doi.org/10.1007/s10570-022-04737-w).
20. E. Grządka, *J. Surfactants Detergents.*, **2012**, *15*, 513–521; [10.1007/s11743-012-1340-5](https://doi.org/10.1007/s11743-012-1340-5).
21. A. Hashim, M. A. Habeeb and Q. M. Jebur, *Egyptian J. Chem.*, **2019**, *62*, 735–749; [https://ejchem.journals.ekb.eg/article\\_60002\\_642c5cdb66830b68322bee2faea4a161.pdf](https://ejchem.journals.ekb.eg/article_60002_642c5cdb66830b68322bee2faea4a161.pdf).
22. H. T. Elhmali, I. Stajcic, A. Stajcic, I. Pesic, M. Jovanovic, M. Petrovic and V. Radojevic, *Polymers*, **2024**; <https://doi.org/10.3390/polym16020278>.
23. A. Abdolmaleki, S. Mallakpour and H. Tabebordbar, *J. Polymer Research.*, **2016**, *23*; [10.1007/s10965-016-1154-7](https://doi.org/10.1007/s10965-016-1154-7).
24. G. Khamidov, Ö. Hazman and I. Erol, *Int. J. Biol. Macromolec.*, **2024**; <https://doi.org/10.1016/j.ijbiomac.2023.128447>.
25. E.-S. Khater, A. Bahnasawy, B. A. Gabal, W. Abbas and O. Morsy, *Scientific Reports*, **2023**; <https://doi.org/10.1038/s41598-023-32218-y>.